Received: 22 April 2020 | Revised: 31 August 2020 | Accepted: 9 September 2020

DOI: 10.1096/fj.202000933RR

RESEARCH ARTICLE

THE FASEB JOURNAL

Phospholipase C beta1 (PI-PLCbeta1)/Cyclin D3/protein kinase C (PKC) alpha signaling modulation during iron-induced oxidative stress in myelodysplastic syndromes (MDS)

Alessandra Cappellini[1] | Sara Mongiorgi[1] | Carlo Finelli[2] | Antonietta Fazio[1] | Stefano Ratti[1] | Maria Vittoria Marvi[1] | Antonio Curti[2] | Valentina Salvestrini[2] | Andrea Pellagatti[3] | Anna Maria Billi[1] | Pann-Ghill Suh[4,5] | James A. McCubrey[6] | Jacqueline Boultwood[3] | Lucia Manzoli[1] | Lucio Cocco[1] | Matilde Y. Follo[1]

[1]Cellular Signalling Laboratory, Department of Biomedical and Neuromotor Sciences, University of Bologna, Bologna, Italy

[2]Department of Hematology and Oncology, Institute of Hematology "L. and A. Seràgnoli, University-Hospital S.Orsola-Malpighi, Bologna, Italy

[3]Blood Cancer UK Molecular Haematology Unit, Nuffield Division of Clinical Laboratory Sciences, Radcliffe Department of Medicine, University of Oxford, and Oxford BRC Haematology Theme, Oxford, UK

[4]Korea Brain Research Institute, Daegu, Republic of Korea

[5]School of Life Sciences, UNIST, Ulsan, Republic of Korea

[6]Department of Microbiology and Immunology, Brody School of Medicine, East Carolina University, Greenville, NC, USA

Correspondence
Lucio Cocco and Matilde Y. Follo, Cellular Signalling Laboratory, Department of Biomedical and Neuromotor Sciences, University of Bologna, via Irnerio 48, 40126, Bologna, Italy.
Email: lucio.cocco@unibo.it (L. C.) and matilde.follo@unibo.it (M. Y. F.)

Funding information
Italian Ministry of Education, University and Research–Research Projects of National Interest; Intesa San Paolo Foundation; Blood Cancer UK, Grant/Award Number: 13042

Abstract

MDS are characterized by anemia and transfusion requirements. Transfused patients frequently show iron overload that negatively affects hematopoiesis. Iron chelation therapy can be effective in these MDS cases, but the molecular consequences of this treatment need to be further investigated. That is why we studied the molecular features of iron effect and Deferasirox therapy on PI-PLCbeta1 inositide signaling, using hematopoietic cells and MDS samples. At baseline, MDS patients showing a positive response after iron chelation therapy displayed higher levels of PI-PLCbeta1/Cyclin D3/PKCalpha expression. During treatment, these responder patients, as well as hematopoietic cells treated with $FeCl_3$ and Deferasirox, showed a specific reduction of PI-PLCbeta1/Cyclin D3/PKCalpha expression, indicating that this signaling pathway is targeted by Deferasirox. The treatment was also able to specifically decrease the production of ROS. This effect correlated with a reduction of IL-1A and IL-2, as well as Akt/mTOR phosphorylation. In contrast, cells exposed only to $FeCl_3$

Abbreviations: Akt, protein kinase B; CI, confidence interval; CTRL, control (untreated cells/samples); DFX, deferasirox; $FeCl_3$, iron(III) chloride; H_2-DCFDA, 2′,7′-dichlorodihydrofluorescein diacetate; HI, hematologic improvement; HRP, horseradish peroxidase; ICT, iron chelation therapy; IL-1A, interleukin 1A; IL-2, interleukin 2; PI, propidium iodide; PI-PLCbeta1, phospholipase C beta 1; PKCalpha, protein kinase C alpha; MDS, myelodysplastic syndromes; mTOR, mechanistic target of rapamycin; NFkB, nuclear factor kappa-light-chain-enhancer of activated B cells; Nox4, NADPH oxidase 4; RBCs, red blood cells; ROS, reactive oxygen species; RPMI, Roswell Park Memorial Institute; WHO, World Health Organization.

Alessandra Cappellini and Sara Mongiorgi equally contributed to this work.

and cells from MDS patients refractory to Deferasirox showed a specific increase of ROS and PI-PLCbeta1/Cyclin D3/PKCalpha expression. All in all, our data show that PI-PLCbeta1 signaling is a target for iron-induced oxidative stress and suggest that baseline PI-PLCbeta1 quantification could predict iron chelation therapy response in MDS.

KEYWORDS
deferasirox, inositides, reactive oxygen species

1 | INTRODUCTION

Nuclear phosphoinositide signaling is implicated in cell proliferation and differentiation.[1-3] Among nuclear inositides, PI-PLCbeta1 is essential for G1/S transition,[4-6] through activation of Cyclin D3 or Diacylglycerol,[7,8] and is implicated in G2/M progression, via Cyclin B1 and PKCalpha.[9,10] The modulation of PI-PLCbeta1 is differentially associated with hematopoiesis in some hematological diseases, such as MDS.[11-13] In fact, not only PI-PLCbeta1 expression in MDS cells is usually increased during myeloid differentiation and is reduced during erythropoiesis,[14,15] but also PI-PLCbeta1 downstream targets are affected. In fact, Cyclin D3 is frequently linked to myeloid induction,[16] whereas the nuclear translocation of PKCalpha is associated with MDS cell cycle arrest and erythroid differentiation.[17] Moreover, PI-PLCbeta1 is interconnected with Akt/mTOR pathway, whose activation is usually linked to leukemogenesis.[12]

Phosphoinositides are strictly correlated with oxidative stress, which can be relevant in cancer, as tumor progression is often accompanied by an increase in ROS and the subsequent DNA damage.[18,19] When used as source of oxidative stress, H_2O_2 is indeed able to induce the synthesis of Phosphatidylinositol-5-phosphate, that becomes a redox-regulated second messenger via Phosphatidylinositol-5-phosphate 4-kinase, possibly affecting chromatin structure or Peptidyl-prolyl cis-trans isomerase NIMA-interacting 1 expression.[20,21] Moreover, ROS formation is associated with an accumulation of Phosphatidylinositol-(3,4,5)-trisphosphate,[22] whose function is related to Phosphatidylinositol-3-kinase, that in turn can activate an oxidant-dependent downstream signaling pathway. In fact, low concentrations of H_2O_2 can regulate cell proliferation or induce mitogenic signaling, by inactivation of Phosphatase and tensin homolog or phosphorylation of Akt.[23]

As for PI-PLCbeta1, it localizes within the nuclear speckles,[13] where also Nox4 can be detected,[24] possibly regulating ROS signaling, especially in MDS. On the one hand, inhibition of Nox4 activity induces a decline of nuclear ROS production.[19] On the other hand, Nox4 co-immunoprecipitates with Matrin 3, a DNA/RNA protein which controls gene expression through interactions with chromatin remodeling.[25] Matrin 3 could, in particular, be a docking site where nuclear ROS signaling may exert its function on transcription/pre-mRNA modulation in specific nuclear domains, such as speckles. Moreover, as Nox4 interacts with Akt pathways,[26] and ROS themselves are associated with PKCalpha signaling,[27] the ROS-dependent nuclear inositide dysregulation could be associated with MDS pathogenesis.[19]

MDS are characterized by ineffective hematopoiesis and cytopenia. Most patients with MDS, at some point in the course of their disease, may require transfusions of RBCs to correct anemia. However, RBCs transfusions contain high levels of iron and the body has no mechanisms to excrete the excess of iron.[28] Excessive iron can then deposit in the tissues and organs, including the liver, heart, endocrine organs, and bone marrow, thus leading to organ damage. Moreover, iron overload may be correlated with malignant progression or with a suppressive effect on MDS hematopoiesis, which is due to the capability of iron-dependent ROS to induce abnormal cell death of both erythroid progenitors and mesenchymal stem cells.[29,30] Increased oxidative stress due to RBCs transfusions is, therefore, a molecular feature of transfusion-dependent MDS,[31-33] that is why iron must be finely regulated in these patients. ICT is referred to drugs that bind circulating and cellular non-transferrin bound iron, removing deposited iron to convert it in a non-toxic molecule and in a form that can be excreted by the body. A consistent, and initially surprising, observation in clinical studies of ICT in MDS is that a significant minority of patients show a clear HI after ICT. These MDS patients also display a reduction of serum ferritin levels and RBCs transfusion requirements that can lead to transfusion independence.[34-36] However, not all MDS patients respond to ICT so brilliantly, and neither all features of iron physiology nor their role in MDS subtypes are completely understood. Therefore, a better clarification of the molecular mechanisms underlying ICT or the detection of new molecular markers able to identify which patients are more or less likely to experience HI with ICT would be helpful in clinical practice.

Among the drugs that can be used for ICT, DFX showed the ability to improve erythropoiesis, by suppressing ROS

TABLE 1 Patients' characteristics

Id	Sex	Age	WHO	K	IPSS	Diagnosis	Interval diagnosis-ICT (months)	Basal RBCU	Basal Ferritin (ng/mL)	Initial Dose (mg/Kg/die)	Duration ICT (Months)	Last Ferritin (ng/mL)	Outcome	Mutated Genes (No. Variants)
1	M	63	RA	46XY	LOW	04/2006	32	63	3770	20	35	571	HI	DDX41 (2)
2	M	72	RARS	46XY	LOW	10/2008	60	>20	1329	10	96	520	HI	TET2 (1)
3	M	78	RARS	46XY	LOW	01/2008	35	42	2151	10	99	572	HI	SF3B1 (1); TP53 (2)
4	M	66	RCMD	46XY	INT 1	01/2007	24	192	1547	10	22	2004	SD	CSF3R (1); NOTCH2 (1); TP53 (1)
5	M	68	RARS	46XY	LOW	11/2009	41	53	2350	5	1	2350	SD	ASXL1 (1); CUX1 (1); ZRSR2 (1)
6	M	61	RA	46XY	LOW	11/2008	552	>20	3580	10	12	3207	SD	NOTCH1 (1); TP53 (2)

Abbreviations: F, female; HI, hematologic improvement; ICT, iron chelation therapy; INT 1, intermediate-1 risk; IPSS, international prognostic scoring system; K, karyotype; LOW, low risk; M, male; RA, refractory anemia; RARS, refractory anemia with ring sideroblasts; RBCU, red blood cells units; RCMD, refractory cytopenia with multilineage dysplasia; SD, stable disease; WHO, World Health Organization.

production, and to induce HI in about 20% MDS patients.[36] Moreover, DFX can specifically affect NFkB expression in human K562 erythroleukemia cells and in MDS patients.[37] In fact, NFkB can be inhibited by 50 μM DFX, but not by either Deferoxamine or Deferiprone,[37] that is, the other two iron chelators frequently used in clinical practice, that usually show lower rates of HI compared to DFX.[28] Other molecular pathways that may be relevant to DFX effect include mTOR signaling, which is important to start protein translation and regulate cell proliferation. Interestingly, upstream mTOR is Akt, and the Akt/mTOR axis has already been associated with PI-PLCbeta1/Cyclin D3/PKCalpha signaling in MDS.[38]

Stemming from these data, here we further investigated the role of DFX therapy in hematopoietic cell lines and in MDS cells, focusing on the effect of DFX on oxidative stress and analyzing the behavior of PI-PLCbeta1, along with its downstream targets Cyclin D3 and PKCalpha. In addition, we tested whether DFX modifies cytokine secretion and Akt/mTOR activation.

2 | MATERIALS AND METHODS

2.1 | Antibodies and reagents

The following antibodies and reagents were purchased from commercial sources. Rabbit anti-PI-PLCbeta1 (#PA5-78439) was from Invitrogen (Waltham, MA, USA), while mouse anti-beta-Actin (#A1978) was from Sigma-Aldrich (St. Louis, MO, USA). Rabbit anti-PKCalpha (#2056), mouse anti-Cyclin D3 (#2936), rabbit anti-Akt (#9272), rabbit anti-phosphorylated-Akt (Ser473, #4058), rabbit anti-mTOR (#2983), rabbit anti-phosphorylated-mTOR (Ser2448, #2971), and the Phototope-HRP Western Blot Detection System (#7071) were from Cell Signaling Technologies (Danvers, MA, USA). Fluorescein isothiocyanate (FITC)-conjugated mouse monoclonal to CD71 was from Santa Cruz Biotechnology (Dallas, TX, USA). Secondary antibodies were HRP-conjugated anti-rabbit IgG (#31460, Thermo Fisher, Waltham, MA, USA), HRP-conjugated anti-mouse IgG (#32430, Thermo Fisher), Alexa Fluor 488-conjugated F(ab')2 fragment of goat anti-mouse IgG (#4408, Cell Signaling Technologies) and Alexa Fluor 488-conjugated F(ab')2 fragment of goat anti-rabbit IgG (#4412, Cell Signaling Technologies). Deferasirox (DFX, #D228650, Toronto Research Chemicals Canada) and $FeCl_3$ (Sigma-Aldrich) were also purchased.

2.2 | Tissue cell cultures

H9C2 rat cardiomyocytes were grown at 37°C with 5% CO_2 in DMEM-high glucose medium (Corning, Manassas,

VA, USA) supplemented with 10% heat-inactivated fetal bovine serum, L-glutamine, and streptomycin/penicillin (Corning). Erythroleukemia K562 and monocytic THP-1 cell lines were grown at 37°C with 5% CO_2 in RPMI 1640 medium (Cambrex BioScience, Baltimore, MD, USA) supplemented with 10% heat-inactivated fetal bovine serum, L-glutamine and streptomycin/penicillin (Corning) at an optimal cell density of 0.3×10^6 to 0.8×10^6 cells/mL. K562 and THP-1 cell lines were treated with 150 μM $FeCl_3$ for 48 hours and DFX 50 μM for 6 hours, used alone or in combination. The in vitro concentration of DFX was used to imitate in vitro the patients' dose. It was calculated considering the common dose range of 10-20 mg/kg/die given to MDS patients. This dose can be increased up to 40 mg/kg or reduced to 5 mg/kg, according to the patient's need.[39] The equivalence between DFX dose and molarity was then calculated considering that the mean weight of 1 mL blood is 1.06 g [40] and that the DFX molecular weight is 373.362 g/mol. This means that the range 5-40 mg/Kg is equal to 14-107 μM. Moreover, pharmacokinetics studies[41] showed that DFX plasma levels are maintained within the therapeutic range over a 24-hour period (20 mg/kg/die give a peak range of 60-100 μmol/L). Therefore, our in vitro experiments were based on the most common dose of 20 mg/kg/die given to our case series. We used a concentration of 50 μM because the same concentration was also used in K562 cells to investigate NFkB signaling and was proven to be effective in K562 experimental model.[37]

2.3 | Patient characteristics, treatment, and evaluation of response

BM samples were obtained from six transfusion-dependent MDS patients treated with DFX and six healthy subjects who had given informed consent according to the Declaration of Helsinki (Table 1). All samples came from the Institute of Hematology "L e A Seràgnoli," University of Bologna, Bologna, Italy. The diagnosis was defined according to the 2008 WHO classification[42] and, according to the International prognostic scoring system,[43] patients were divided into low risk (n = 5) or intermediate risk (n = 1). Response to treatment and the clinical outcome were evaluated according to the revised International Working Group response criteria.[44] Before the therapy, all patients were transfusion-dependent (ie, requiring ≥1 unit of packed RBCs in ≤8 weeks averaged over 4 months before the start of treatment) and had a serum ferritin level ≥1000 ng/mL.[34] Patients were treated with the iron chelator DFX (oral administration), with a 10-20 mg/kg/die starting dose range that could be personalized according to their blood transfusion frequency, with the aim to reduce transfusion-dependent iron overload.[34]

2.4 | Isolation of mononuclear cells

For in vitro experiments, BM mononuclear cells (MNCs) were isolated at baseline and during therapy by Ficoll-Paque density-gradient centrifugation (Amersham Biosciences, Uppsala, Sweden), according to the manufacturer's instructions. All analyses were performed on samples from patients at the time of diagnosis and during the therapy.

2.5 | Illumina next generation sequencing

The mutational profile of 32 recurrently mutated genes in myeloid malignancies was determined using an Illumina TruSeq Custom Amplicon next-generation sequencing gene panel and the TruSeq Amplicon 2.0 BaseSpace app workflow[45] (Illumina, San Diego, CA, USA), as previously described.[46]

2.6 | Gene and protein expression analysis

Total RNA was extracted from cell lines and patients' samples. RNA was retro-transcribed and the expression of PI-PLCbeta1, Cyclin D3 and PKCalpha genes was assessed using a standard TaqMan Real-Time PCR method (Applied Biosystems, Foster City, CA, USA), with the Glyceraldehyde 3-phosphate dehydrogenase TaqMan probe as the endogenous control and a pool of healthy subjects as an internal control, as previously reported.[47] Protein amount was quantified on hematopoietic cell lines by Western Blot analyses, using beta-Actin as a control of equal protein loading, as already described,[16] and immunocytochemistry. For MDS samples, as the number of patients' cells was limited, protein expression was determined by immunocytochemistry only, as previously illustrated.[15]

2.7 | Flow cytometric analysis of cell cycle and apoptosis

Cell cycle distribution of hematopoietic cell lines was examined according to Poli et al,[17] while apoptosis was quantified by staining with Annexin V/Alexa Fluor 488 and PI, following the manufacturer's instructions (Alexa Fluor 488 Annexin V/Dead cell apoptosis kit; #V13245, Invitrogen). The percentage of apoptotic cells was also detected on a PI histogram (FL3lin/count) as a hypo-diploid peak using a suitable acquisition software (CXP Cytometer, Beckman Coulter, Brea, CA, USA) and a proper software analysis (CXP Analysis, Beckman Coulter). For a more accurate evaluation of primary necrotic cells, non-permeabilized Annexin-V stained cells were counter-stained with PI.

2.8 | Flow cytometric detection of CD71 levels

For the detection of CD71 surface antigen, K562 cells were cultivated in RPMI medium (Cambrex Bio Science) and H9C2 cells in DMEM-high glucose (Corning). The percentage of positive cells was quantified using an FC500 Dual Laser Flow Cytometer with the appropriate software (System II, Beckman Coulter), as reported elsewhere.[17] At least 10 000 events/sample were acquired.

2.9 | Flow cytometric analysis of ROS production

Intracellular ROS production was monitored by oxidation of a fluorescein reduced derivative probe, used as living cell-permeant indicator (H_2-DCFDA; #C400, Invitrogen). Under the influence of intracellular esterases, this probe becomes sensitive to ROS-induced oxidation, resulting in an increased green fluorescence, detectable by a flow cytometer equipped with a 488 nm Argon Laser as excitation source and appropriate filters for fluorescein isothiocyanate (emission on wavelength 517-527 nm). At first, 8×10^5 K562 or THP-1 cells were incubated with $FeCl_3$ for 48 hours ($FeCl_3$) or left untreated (CTRL). Then, to remove RPMI Medium's Red Phenol and any iron residues (that can virtually interfere with intensity of fluorescent signal), samples were briefly centrifuged (1200 rpm × 8 minutes), washed twice in 1x phosphate buffered saline, resuspended in 1 mL of 1x phosphate buffered saline and added with 5 μM H_2-DCFDA. For both CTRL and $FeCl_3$ cells, we collected four samples with 8×10^5 cells each: one to assess the cells' autofluorescence (AUTO, to be used as an internal control), one to evaluate the baseline ROS activity (CTRL or $FeCl_3$), one to be used as a positive control of ROS production (H_2O_2, with cells treated with15 μM H_2O_2 for 5 hours) and one to test the effect of treatment (DFX, with cells treated with 50 μM DFX for 6 hours). For the autofluorescence samples, a natural-baseline, not probe-induced, green fluorescence was used. CTRL and $FeCl_3$ samples were incubated at 37°C for 10 minutes, to induce the probe to enter the cells. After this probe-loading phase, cells were treated with DFX and/or with H_2O_2. Samples were then incubated for 6 hours in the dark at 37°C before undergoing the cytofluorimetric analysis. To ensure the correct incoming of the probe in cells, the FL1 green photomultiplier voltage was set to have the autofluorescence signal within the first scale decade (log scale), so that the ROS basal production appeared as a histogram's right-shift of at least 2.5 decades.

2.10 | Cytokine secretion

The profile of multiple cytokines secreted by stimulated cells was tested using the Multi-Analyte ELISArray Kit (Qiagen, Venlo, The Netherlands), according to the manufacturer's instructions.

2.11 | Statistical analyses

All the analyses were performed using the GraphPad Prism Software (v.4.0, La Jolla, CA, USA). Dunnett's test post-analysis of variance was used to compare continuous values and paired Student *t* test was used to compare paired groups. Tests were considered statistically significant when the *P*-value was $<.05$.

3 | RESULTS

3.1 | Effect of $FeCl_3$ on K562 and THP-1 cell cytotoxicity

To determine the right concentration of $FeCl_3$ for our experimental model, a dose response analysis on K562 and THP-1 cells was performed, and an Annexin V/PI evaluation was carried out (Figure 1). Since previous works on cardiac cells showed that the oxidative effect of $FeCl_3$ was detectable after treatment with 150 μM for 48 hours,[48] we also started with a 48 hours treatment and with doses under and above 150 μM. In K562 cells (Figure 1A,C), $FeCl_3$ 150 μM for 48 hours was able to induce a mild early apoptosis (5.9% of Annexin V+/PI- cells), a mild late apoptosis (2.6% of Annexin V+/PI+ cells) and a mild necrosis (2.2% of Annexin V-/PI+ cells). At lower concentrations (100 μM) there was no statistical difference with control cells, whereas at higher concentrations (1 mM and 5 mM), both apoptotic and necrotic fractions increased. In contrast, as shown in Figure 1B,D, THP-1 cells seemed to be significantly affected only by high concentrations of $FeCl_3$ (ie, 5 mM).

3.2 | Effect of $FeCl_3$ and DFX on K562 and THP-1 cell cycle and apoptosis

To mimic the iron accumulation induced by transfusions, K562 and THP-1 cells were treated with 150 μM $FeCl_3$ for 48 hours, while DFX was used at a concentration of 50 μM for 6 hours.

Cells were treated with $FeCl_3$ and DFX alone or in combination, and both cell cycle and Annexin V/PI analyses were performed (Figures S1 and S2). In both cell lines, the selected doses of $FeCl_3$ and DFX did not have significant effects on cell cycle or apoptosis. Indeed, in K562 cells, $FeCl_3$, alone or in combination with DFX, was able to induce a small increase in the number of sub-G0/G1 cells (4.2% $FeCl_3$/$FeCl_3$ + DFX vs 2.0% CTRL), while all of the other cell cycle phases were

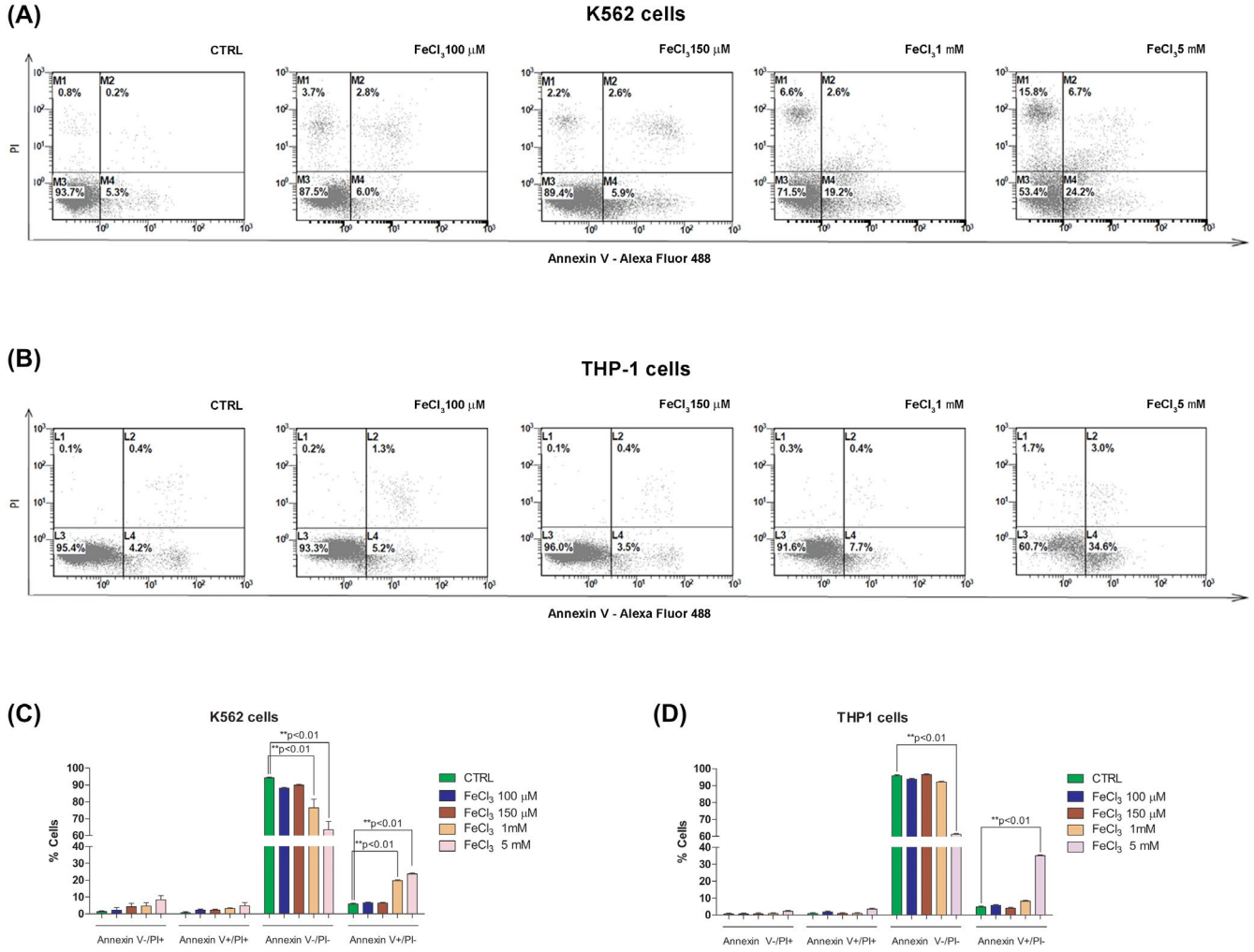

FIGURE 1 Effect of $FeCl_3$ exposition on cytotoxicity of K562 and THP-1 cells. Flow cytometric analysis of (A) K562 and (B) THP-1 cells stained with Annexin V/PI after exposition of 48 hours with increasing doses of $FeCl_3$ for up to 5 mM (as indicated). Dot plots report the cell percentage for each quadrant. In K562 cells, $FeCl_3$ 150 μM for 48 hours was able to induce a mild early apoptosis (5.9% of Annexin V+/PI- cells), a mild late apoptosis (2.6% of Annexin V+/PI+ cells) and a mild necrosis (2.2% of Annexin V-/PI+ cells). In contrast, THP-1 cells seemed to be significantly affected only by high concentrations of $FeCl_3$ (ie, 5 mM). Percentage of PI+/Annexin V- cells are indicated in upper left corner; PI+/Annexin V+: upper right corner; PI-/Annexin V+: lower right corner; PI-/Annexin V-: lower left corner. Representative data of at least three independent experiments. C, Statistical analysis of Annexin V/PI results in K562 cells show that there is a statistically significant difference in Annexin V-/PI- fractions and Annexin V+/PI- fractions only after treatment with $FeCl_3$ 1mM and 5mM, as compared with CTRL cells (**$P < .01$ vs CTRL), whereas in (D) THP-1 cells there is a statistically significant difference in Annexin V-/PI- fractions and Annexin V+/PI- fractions only after treatment with $FeCl_3$ 5mM, as compared with CTRL cells (**$P < .01$ vs CTRL). Data are representative of at least three independent experiments

not significantly different from the untreated cells. In contrast, DFX alone induced a prominent G0/G1 arrest (49.6% DFX vs 36.0% CTRL), that was not detectable in K562 cells after the combination treatment (Figure S1A,C). As for Annexin V/PI analyses, neither $FeCl_3$ nor DFX, used alone or in combination, were able to induce a major change in apoptotic or necrotic cells (Figure S1B,D). In fact, the early apoptotic (Annexin V+/PI-) fractions showed a minimal reduction only in K562 cells treated with DFX (2.3% DFX vs 4.3% CTRL), while both $FeCl_3$ alone and the combination treatment showed comparable levels of early apoptotic cells (4.2% and 5.2%, respectively, vs 4.3% CTRL). Moreover, only in $FeCl_3$-treated cells, the necrotic (Annexin V-/PI+) fraction increased more than the other samples, although not reaching a statistically significant difference (3.9% $FeCl_3$ vs. 1.4% CTRL). Conversely, although DFX, in combination with $FeCl_3$, was able to induce a mild, not statistically significant, increase of the THP-1 early apoptotic cell fraction (Figure S2B,D), this was not correlated to substantial changes in cell cycle profile (Figure S2A,C).

3.3 | Effect of $FeCl_3$ and DFX on induction of ROS in K562 and THP-1 cells

To examine the effect of $FeCl_3$ and DFX on oxidative stress, we optimized a flow cytometric-based test (Figures 2 and 3),

using autofluorescence (AUTO) as a reference marker (Figures 2G and 3G). At first, we compared the ROS production in K562 untreated samples (CTRL, Figure 2A) with cells treated with $FeCl_3$ only ($FeCl_3$, Figure 2B), finding out that the $FeCl_3$ stimulus was able to increase the ROS production by about 14% (38.82% CTRL vs 53.02% $FeCl_3$). Instead, DFX was able to reduce the ROS production in both CTRL cells (38.82% CTRL vs 0.05% DFX, Figure 2C) and in $FeCl_3$-treated cells (53.02% $FeCl_3$ vs 0.58% $FeCl_3$ + DFX, Figure 2D). Interestingly, the decrease in ROS production was higher in $FeCl_3$-pretreated cells, as the difference corresponded to 52.44%, while in CTRL cells it was reduced by 38.77%. Finally, the exposition to H_2O_2 represented the positive control in both experimental conditions, as H_2O_2 was able to induce the ROS production by about 60% in the CTRL samples (38.82% CTRL vs 99.01% H_2O_2, Figure 2E) and by about 45% in the $FeCl_3$-treated cells (53.02% $FeCl_3$ vs 98.39% $FeCl_3$ + H_2O_2, Figure 2F).

In THP-1 cells, $FeCl_3$ was not able to induce ROS production, rather the opposite: $FeCl_3$ was indeed associated with a decrease of ROS production (51.40% CTRL vs 38.00% $FeCl_3$, Figure 3A,B). Even DFX was able to reduce the ROS production, in both CTRL (51.40% CTRL vs 0.20% DFX, Figure 3C) and $FeCl_3$-treated cells (38.00% $FeCl_3$ vs 5.50% $FeCl_3$ + DFX, Figure 3D). As shown in Figure 3E,F, the exposition to H_2O_2 represented the positive control in both experimental conditions, as H_2O_2 was able to induce the ROS production by about 45% in the CTRL samples (51.40% CTRL vs 97.10% H_2O_2, Figure 3E) and by about 60% in the $FeCl_3$-treated cells (38.00% $FeCl_3$ vs 98.70% $FeCl_3$ + H_2O_2, Figure 3F).

As a further control, we also tested the effect of three concentrations of DFX in CTRL and H_2O_2-treated K562 cells, using the autofluorescence (AUTO) as a reference (Figure S3G). Again, DFX was able to reduce the ROS production in a dose-dependent manner, although there was no significant difference between DFX 50 and 75 μM (Figure S3A,C,E). In contrast, increasing doses of DFX added to H_2O_2 were only able to partially affect H_2O_2-induced ROS

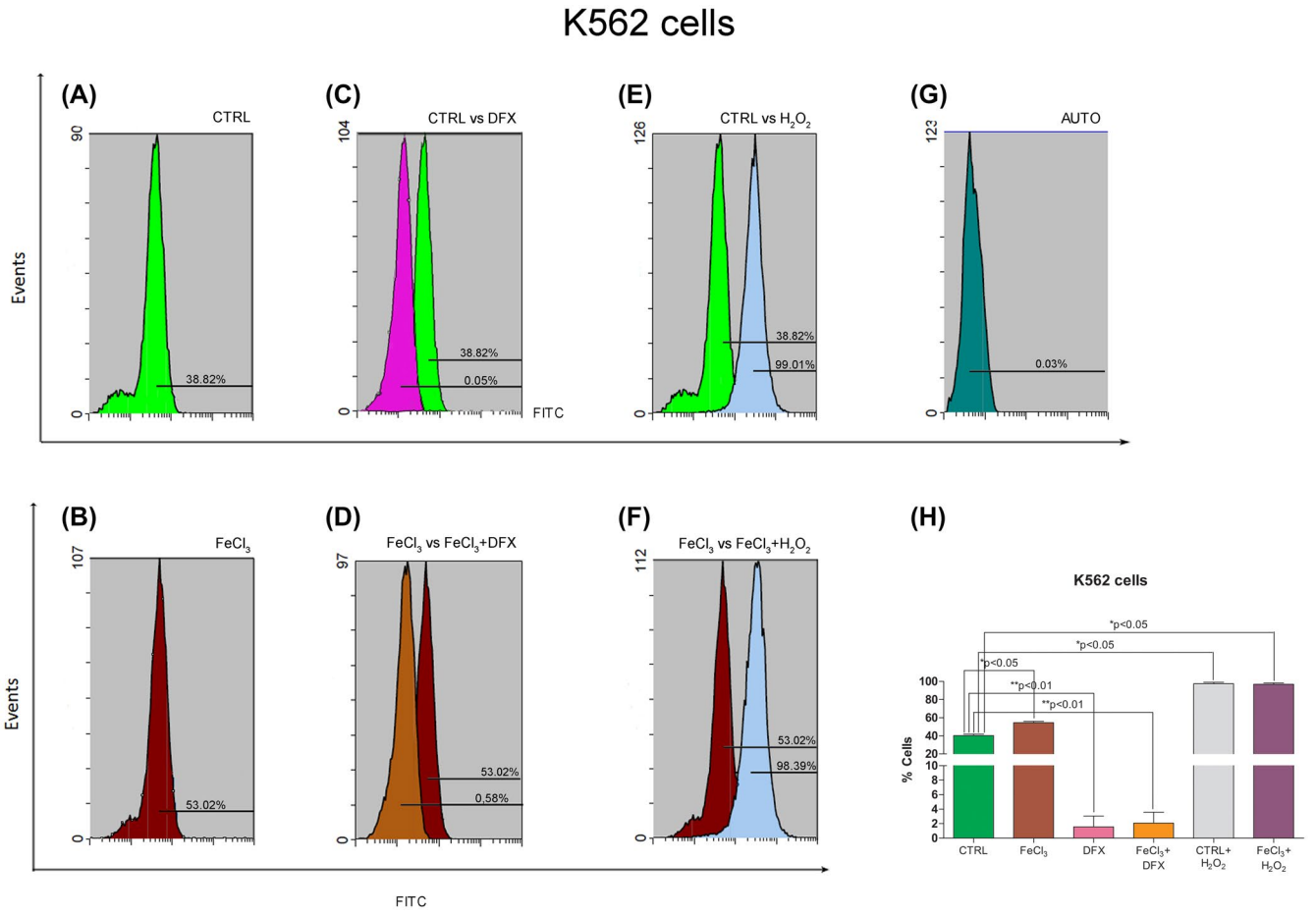

FIGURE 2 Effect of $FeCl_3$ and DFX exposition on ROS production of K562 cells. The ROS production in (A) K562 untreated samples (CTRL) was compared with (B) cells pre-treated with $FeCl_3$ only ($FeCl_3$). $FeCl_3$ is able to induce the ROS production by about 14% (53.02% CTRL vs 38.82% $FeCl_3$). DFX reduces the production of ROS in both samples: in (C) CTRL cells, ROS production was reduced by 38.77%, while in (D) $FeCl_3$-pretreated cells the difference corresponded to 52.44%. (E, F) H_2O_2 induces ROS production in both samples. Representative data of at least three independent experiments. (G) Autofluorescence graph (AUTO), used as a reference marker for all analyses. (H) Statistical analysis of ROS production in K562 cells (*$P < .05$; **$P < .01$). Data are representative of at least three independent experiments

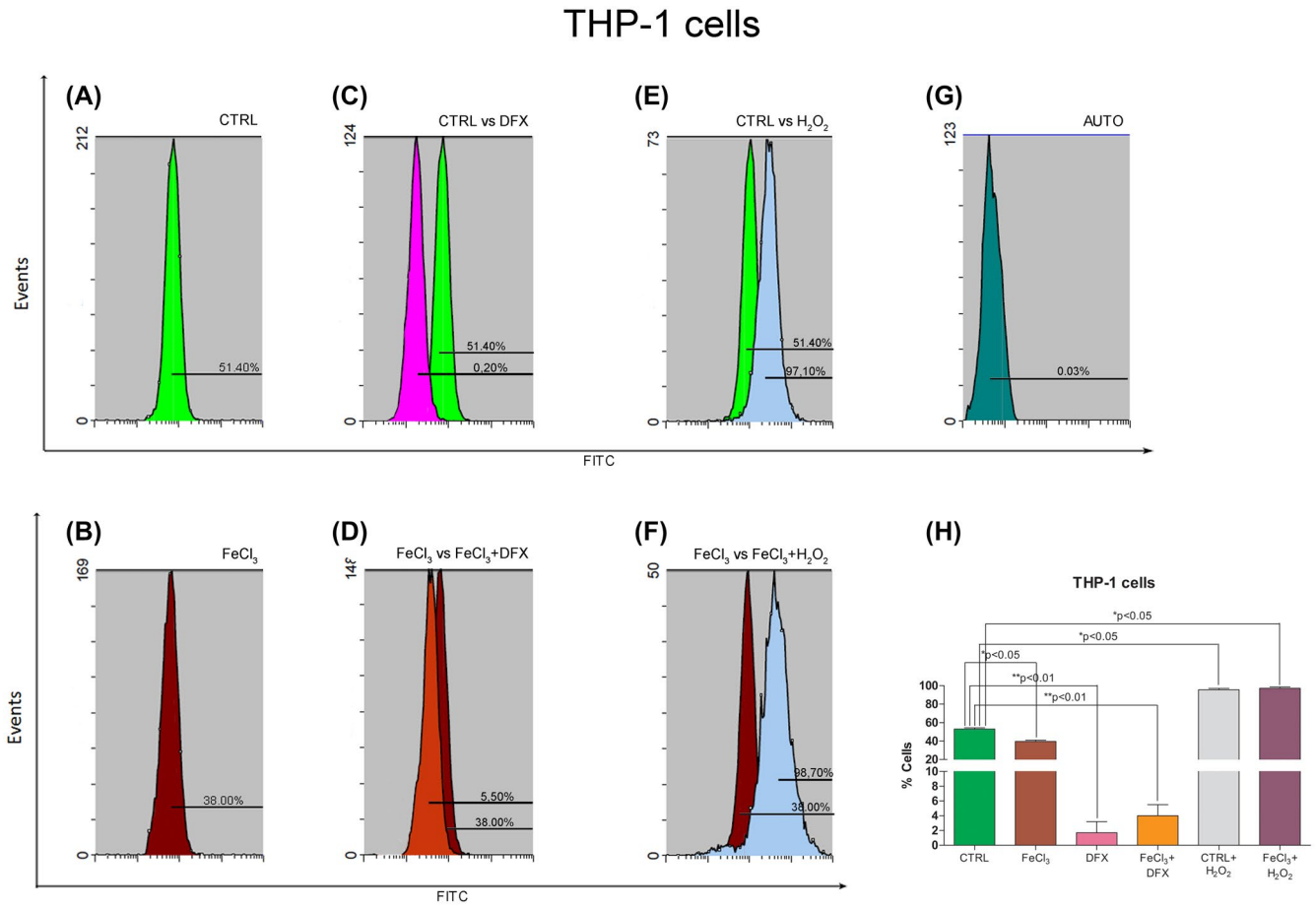

FIGURE 3 Effect of $FeCl_3$ and DFX exposition on ROS production of THP-1 cells. The ROS production in (A) THP-1 untreated samples (CTRL) was compared with (B) cells pre-treated with $FeCl_3$ only ($FeCl_3$). $FeCl_3$ is not able to induce ROS production, rather the opposite (38.00% CTRL vs 51.40% CTRL + $FeCl_3$). Even DFX and H_2O_2 treatments are able to induce a response in both samples: (C, D) DFX reduces the production of ROS, whereas (E, F) H_2O_2 induces it. Representative data of at least three independent experiments. G, Autofluorescence graph (AUTO), used as a reference marker for all analyses. H, Statistical analysis of ROS production in K562 cells (*$P < .05$; **$P < .01$). Data are representative of at least three independent experiments

production (Figure S3B,D,F). This was evident from the analysis of the mean fluorescence intensity reported in Figure S3H. Finally, also the expression of the CD71 surface marker was analyzed during DFX treatment, but no significant changes were detected among the different concentrations tested, while all K562 samples showed a CD71 percentage significantly higher than both autofluorescence (AUTO), used as a reference marker, and H9C2 cells, representing our negative control (Figure 4).

3.4 | Effect of $FeCl_3$ and DFX on gene and protein expression of PLCbeta1/Cyclin D3/PKCalpha signaling in K562 cells

As Figure 5A shows, the amount of PI-PLCbeta1 gene expression was significantly increased in K562 cells exposed to $FeCl_3$, as compared with baseline (Student's *t* test, $P < .05$ vs. baseline, 95% CI +0.08 to +1.19), while it was almost constant, or slightly decreased, in K562 cells treated with the combination of $FeCl_3$ and DFX, as compared with baseline (Student's *t* test, $P > .05$ vs. baseline, 95% CI −0.52 to +0.58). Even Cyclin D3 gene expression showed an increase, although not statistically significant, in $FeCl_3$-treated K562 cells, as compared with baseline (Student's *t* test, $P > .05$ vs. baseline, 95% CI +0.11 to +0.79), but the combination of $FeCl_3$ and DFX showed a statistically significant reduction of Cyclin D3 mRNA (Student's *t* test, $P < .05$ vs. baseline, 95% CI −0.20 to −1.11). Finally, even PKCalpha expression was significantly increased in K562 cells treated with $FeCl_3$ (Student's *t* test, $P < .05$ vs. baseline, 95% CI +0.37 to +2.97), while K562 cells exposed to the combination treatment showed a slight decrease, as compared with baseline (Student's *t* test, $P > .05$ vs. baseline, 95% CI −1.02 to +1.57). Protein expression analysis confirmed the mRNA behavior: PI-PLCbeta1/Cyclin D3/PKCalpha axis was induced in $FeCl_3$-treated cells, while the treatment with DFX or $FeCl_3$ + DFX resulted in a reduction of protein expression

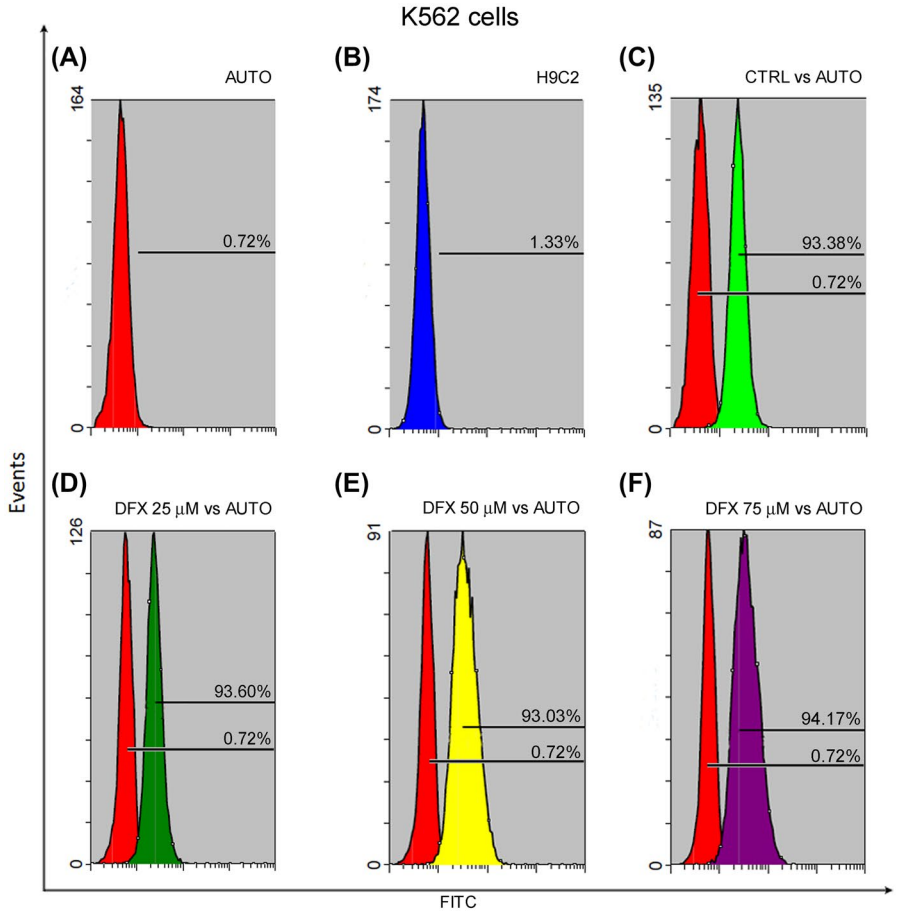

FIGURE 4 Effect of DFX on the expression of CD71 erythoid-specific surface markers in K562 cells. Flow cytometric analysis of surface CD71 expression in K562 cells treated with increasing doses of DFX. Representative data of at least three independent experiments. A, Autofluorescence (AUTO) and (B) H9C2 cells were used as a reference marker and a negative control, respectively. C, Overlay between untreated (CTRL) K562 cells and AUTO: 93.38% CTRL cells are positive for CD71. D, Overlay between K562 cells treated with DFX 25 µM and AUTO: 93.36% DFX 25 µM cells are positive for CD71. E, Overlay between K562 cells treated with DFX 50 µM and AUTO: 93.03% DFX 50 µM cells are positive for CD71. F, Overlay between K562 cells treated with DFX 75 µM and AUTO: 94.17% DFX 75 µM cells are positive for CD71. G, Statistical analysis of CD71 expression in K562 cells during treatment (**$P < .01$). Data are representative of at least three independent experiments

(Figure 5B-D). As for the inositide localization, all tested proteins were mostly cytoplasmic at baseline, and expressed both in nucleus and cytoplasm during treatment.

3.5 | Effect of $FeCl_3$ and DFX on cytokine secretion in K562 cells

K562 cells were treated with $FeCl_3$ and DFX, alone or in combination, and the therapy effect on the expression of 12 cytokines commonly secreted by hematopoietic cells was analyzed. As Figure 6A shows, ten cytokines showed similar or not statistically significant reducing levels during any treatment, as compared with baseline. Conversely, two cytokines were differentially expressed during $FeCl_3$ and DFX administration (Figure 6B): $FeCl_3$ alone was able to greatly induce both IL-1A and IL-2 secretion, while both DFX alone and the combination of $FeCl_3$ and DFX induced a reduction of the secretion of these cytokines. As Figure 6B shows, this decrease reached a statistically significant difference only after exposition to DFX alone, while it was close to significant after $FeCl_3$ and DFX combination treatment ($P = .05$ for IL-1A, $P = .06$ for IL-2).

3.6 | Effect of $FeCl_3$ and DFX on Akt/mTOR protein expression in K562 cells

The treatment with DFX, alone or in combination with $FeCl_3$, specifically reduced the expression of the phosphorylated isoforms of Akt and mTOR, with a more marked decrease

in phosphorylated-mTOR. In contrast, $FeCl_3$ alone was able only to marginally induce the specific activation of both proteins, as compared with the untreated (CTRL) cells. The total proteins were not affected, and Beta-Actin was used as a loading control (Figure 6C).

3.7 | Patient outcomes and gene mutation status

Between April 2006 and December 2019, six patients with lower risk MDS started ICT with DFX. They were

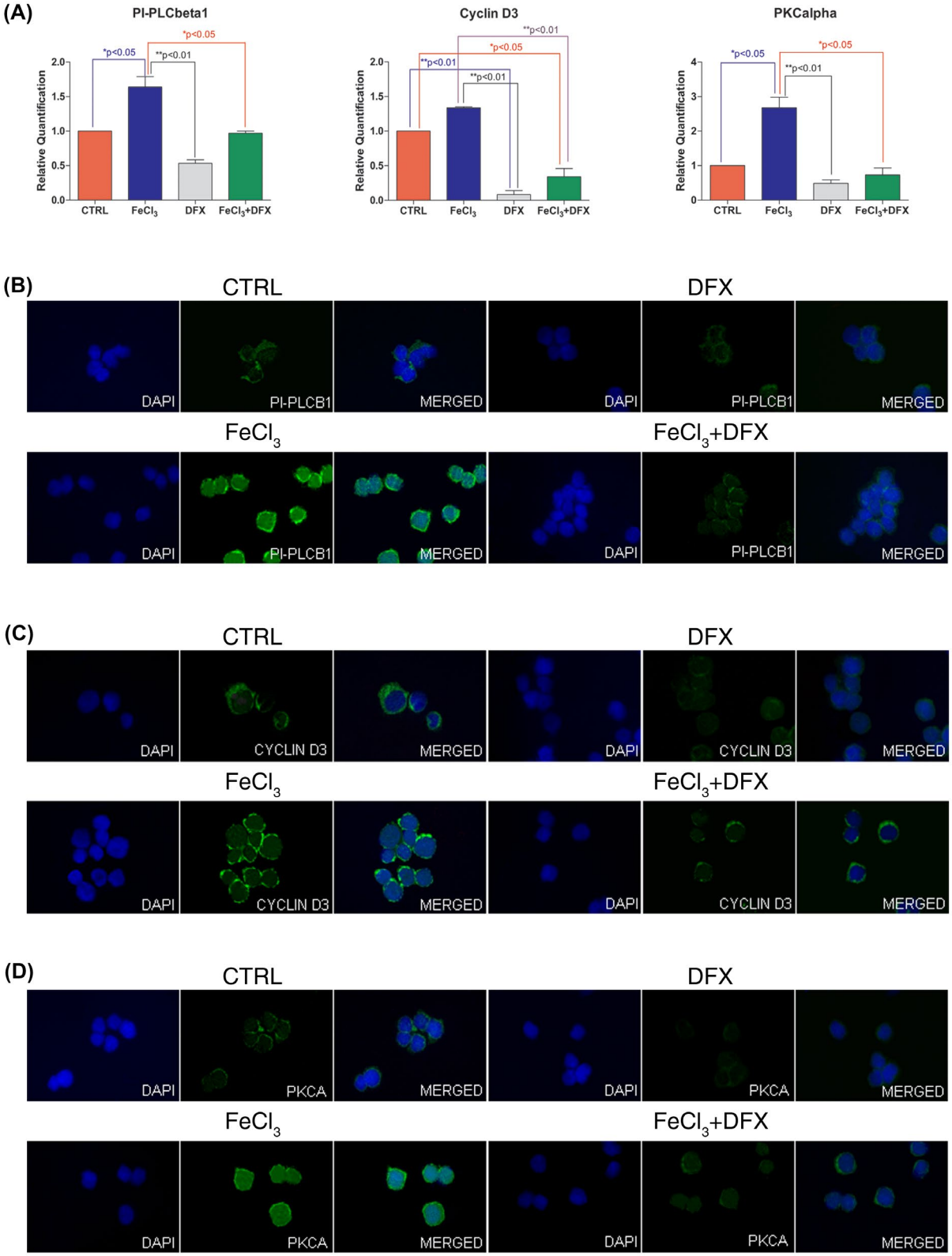

FIGURE 5 Gene and protein expression of PI-PLCbeta1, Cyclin D3, and PKCalpha in K562 cells during $FeCl_3$ and DFX exposition. K562 cells were treated with 150 μM $FeCl_3$ for 48 hours and/or 50 μM DFX for 6 hours. A, The amount of PI-PLCbeta1, Cyclin D3 and PKCalpha gene expression increases in K562 cells exposed to $FeCl_3$ ($FeCl_3$), as compared with baseline (CTRL), while it is almost constant, or decreased, in K562 cells treated with DFX (DFX) or the combination of $FeCl_3$ and DFX ($FeCl_3$ + DFX), as compared with baseline (CTRL). Data are representative of at least three independent experiments (*$P < .05$; **$P < .01$). B, Representative immunocytochemical analysis of PI-PLCbeta1 protein expression (green signal) in K562 cells during $FeCl_3$ and DFX treatment. Only $FeCl_3$-treated cells show an increase of protein expression during therapy. Original magnification ×600. Nuclei are visualized by DAPI staining (blue signal). At least 10 different fields were observed. C, Representative immunocytochemical analysis of Cyclin D3 protein expression (green signal) in K562 cells during $FeCl_3$ and DFX treatment. Original magnification ×600. Nuclei are visualized by DAPI staining (blue signal). Only $FeCl_3$-treated cells show an increase of protein expression during therapy. D, Representative immunocytochemical analysis of PKCalpha protein expression (green signal) in K562 cells during $FeCl_3$ and DFX treatment. Only $FeCl_3$-treated cells show an increase of protein expression during therapy. Original magnification ×600. Nuclei are visualized by DAPI staining (blue signal). At least 10 different fields were observed

transfusion-dependent (median number of RBC units at baseline: 58) and showed a baseline median ferritin level of 2250.5 ng/mL (range 1547-3770 ng/mL). With a median follow-up of 40.5 months (range 2-99 months), three patients showed a significant improvement of hematopoiesis (defined as HI, according to the International Working Group response criteria[44]). Following hematologic response, these patients also became transfusion independent and continued DFX until the achievement of a serum ferritin level <500 ng/mL. In contrast, the other three patients did not show any HI and remained transfusion-dependent during DFX administration, thus showing a persistently high ferritin level (Table 1).

Next generation sequencing analysis carried out on samples at baseline (Table 1) are in accordance with a recent analysis where no single baseline gene mutation was predictive of HI, but the mutation number was lower in DFX responders compared to resistant patients.[49]

3.8 | PI-PLCbeta1, Cyclin D3, and PKCalpha gene and protein expression levels in MDS patients treated with DFX

At baseline, the level of PI-PLCbeta1, Cyclin D3, and PKCalpha mRNA in BMMNCs from three patients who subsequently showed a hematologic response after ICT (ie, responders) was higher as compared with non-responders and with a pool of healthy subjects (Figure 7A). During DFX therapy, the amount of PI-PLCbeta1 mRNA significantly increased in non-responder patients, as compared with baseline (Student's *t* test, $P < .05$ vs. baseline, 95% CI +1.39 to +2.27), while in responder patients it remained substantially unchanged (Student's *t* test, $P > .05$ vs. baseline, 95% CI −0.20 to +0.52). Cyclin D3 gene expression showed a similar behavior: during DFX therapy, Cyclin D3 mRNA significantly increased in non-responder patients, as compared with baseline (Student's *t* test, $P < .05$ vs. baseline, 95% CI +0.10 to +2.00), while responder patients showed an almost constant Cyclin D3 level (Student's *t* test, $P > .05$ vs. baseline, 95% CI −0.95 to +0.73). Finally, even PKCalpha significantly increased only in non-responder patients (Student's *t* test, $P < .05$ vs. baseline, 95% CI +2.40 to +2.92), while responder patients showed a decrease, although not statistically significant (Student's *t* test, $P > .05$ vs. baseline, 95% CI −0.72 to −0.30). Protein expression analysis confirmed the mRNA behavior: after ICT, PI-PLCbeta1, Cyclin D3, and PKCalpha expression were highly induced in non-responder subjects, while the same proteins did not significantly change in responder patients (Figure 7B-D). Moreover, all analyzed proteins seemed to show a localization change during therapy, that was more evident for PKCalpha, which seemed to be localized both in nucleus and cytoplasm during therapy.

4 | DISCUSSION

Nuclear inositide-dependent signaling is finely regulated in the hematopoietic system and is involved in MDS pathogenesis, through genetic and epigenetic processes.[50-52] PI-PLCbeta1 is particularly implicated in cell cycle regulation and differentiation, via Cyclin D3 and PKCalpha. Moreover, given its nuclear co-localization with Nox4,[24] PI-PLCbeta1 could play a relevant role in oxidative stress.

MDS patients are frequently dependent on blood transfusions. This can lead to an exogenous iron overload that may be highly cytotoxic, through the production of ROS. That is why MDS patients requiring blood transfusions need to be treated with iron chelators, that is, DFX. Although the mechanism of action of DFX is well known (two molecules of DFX bind one molecule of Fe^{3+} to form a stable complex which is eliminated via the kidneys), the molecular effects of ICT are still not fully clarified.

That is why in this study we examined more in detail the molecular mechanisms underlying the effect of DFX on PI-PLCbeta1 signaling, using both hematopoietic cells and MDS samples as experimental models. At first, we tested K562 and THP-1 cells, that is, a erythroleukemia cell line that has been recently used to analyze the effect of DFX[53] and a monocytic cell line often used in inositide studies. We did not test any other erytholeukemia cell line, as other papers

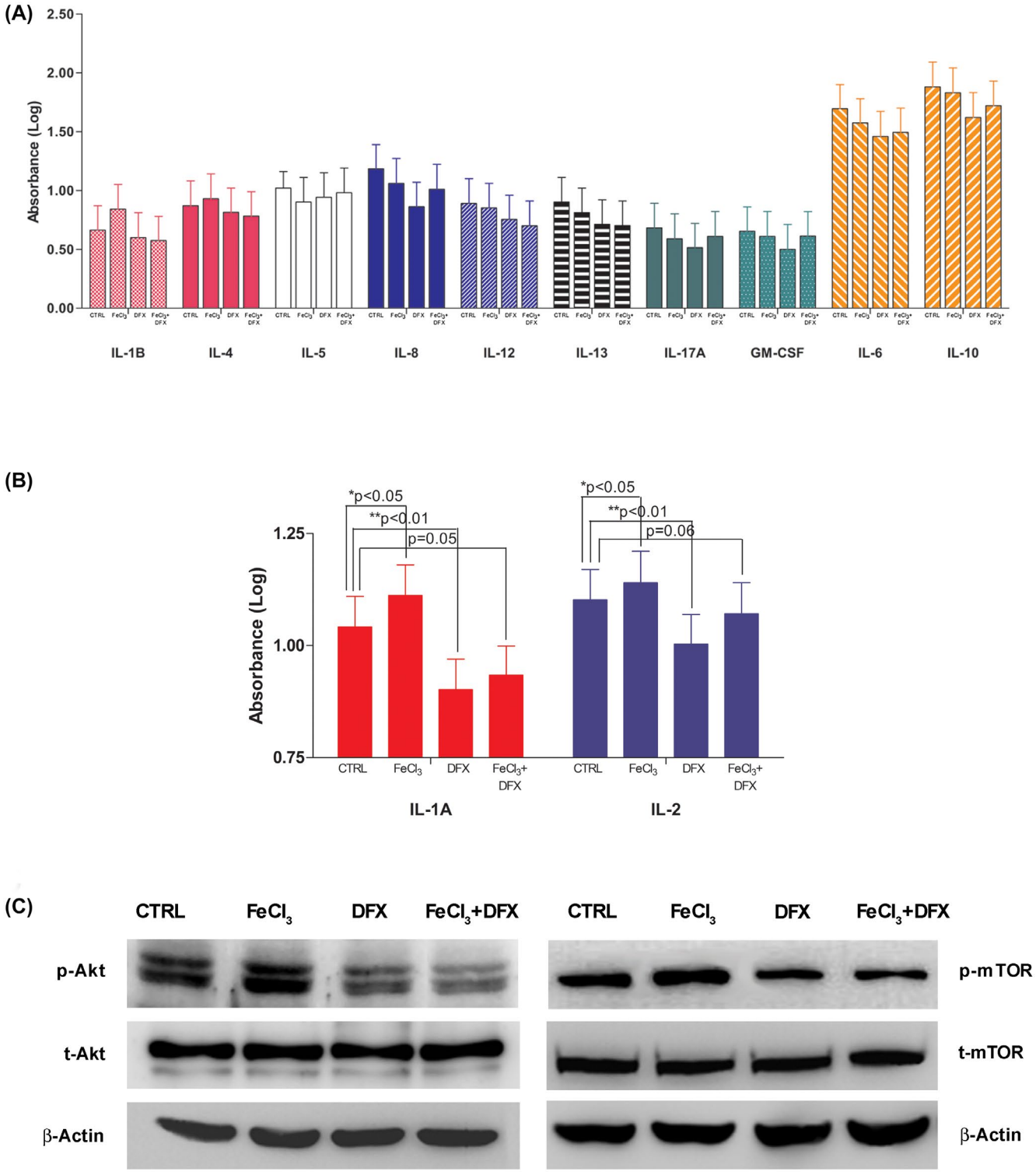

FIGURE 6 Effect of $FeCl_3$ and DFX on cytokine secretion and Akt/mTOR protein expression in K562 cells. K562 cells were treated with 150 μM $FeCl_3$ for 48 hours ($FeCl_3$) or 50 μM DFX for 6 hours (DFX) alone, or in combination ($FeCl_3$ + DFX), and the therapy effect on the secretion of 12 cytokines was analyzed and compared with untreated (CTRL) cells. A, Ten cytokines show similar or slightly, not statistically significant, reduced levels during treatment, while (B) IL-1A and IL-2 are differentially expressed during $FeCl_3$ and DFX administration: $FeCl_3$ alone is able to induce both cytokines in a statistically significant manner, as compared with untreated cells (CTRL), while DFX, alone or in combination with $FeCl_3$, induces a reduction of cytokine secretion. The decrease in IL-1A and IL-2 is statistically significantly only after exposition to DFX alone (*$P < .05$), while it is close to significant after $FeCl_3$ and DFX combination ($P = .05$ for IL-1A and $P = .06$ for IL-2). Data are representative of at least three independent experiments (*$P < .05$; **$P < .01$). C, Protein expression of total and phosphorylated Akt and mTOR show that the treatment with DFX alone or the combination of $FeCl_3$ and DFX corresponds to a lower amount of both phosphorylated proteins, as compared with the total proteins and the untreated (CTRL) cells. In contrast, $FeCl_3$ alone was able only to marginally induce the specific activation of both proteins. Beta-Actin is used as a loading control

dealing with ROS studies showed similar effects on K562 and TF-1 cells,[54] and because our main interest in this study was about the involvement of inositides in oxidative stress during DFX therapy. As previous reports showed that the addition of iron chelators to cell cultures exposed to $FeCl_3$ was able to counteract its cytotoxic effect,[55] and given that DFX has a strong affinity for Fe^{3+}, we used $FeCl_3$ as a source of iron, to mimic the effect of MDS iron overload due to RBCs transfusions. Our results show that the selected concentrations of $FeCl_3$ and DFX did not significantly affect cell cycle, nor apoptosis, in both cell lines. Therefore, we hypothesized that the prevalent effect of our experimental conditions was on induction of oxidative stress and not of cytotoxicity. That is why we then optimized a flow cytometric-based protocol aiming to determine the amout of ROS production in our cells. When $FeCl_3$-pretreated K562 cells were labeled with

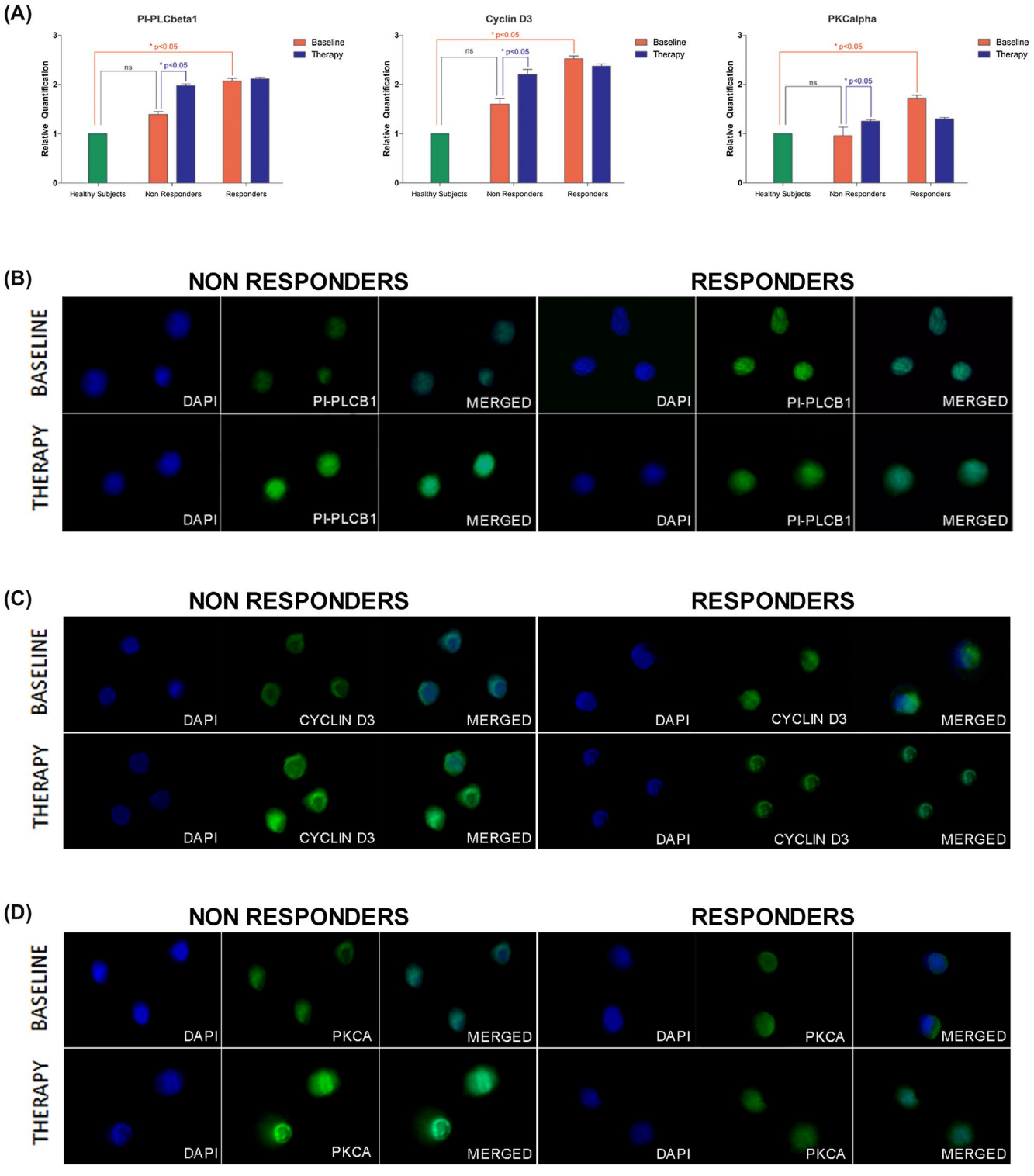

FIGURE 7 Gene and protein expression of PI-PLCbeta1, Cyclin D3, and PKCalpha in MDS patients during DFX therapy. A, At baseline, only responder patients show higher, statistically significant, levels of PI-PLCbeta1, Cyclin D3 and PKCalpha mRNAs, as compared with non-responder patients and healthy subjects. During DFX therapy, non-responder patients show a statistically significant increase of PI-PLCbeta1, Cyclin D3 and PKCalpha gene expression, as compared with baseline and responder patients. Data are representative of at least three independent experiments. (*$P < .05$ vs Healthy Subjects or Baseline; ns: not statistically significant). B, Representative immunocytochemical analysis of PI-PLCbeta1 protein expression (green signal) in responder and non-responder MDS patients during DFX therapy. Only non-responders show an increase of protein expression during therapy. Original magnification ×600. Nuclei are visualized by DAPI staining (blue signal). At least 10 different fields were observed. C, Representative immunocytochemical analysis of Cyclin D3 protein expression (green signal) in responder and non-responder MDS patients during DFX therapy. Original magnification ×600. Nuclei are visualized by DAPI staining (blue signal). Only non-responders show an increase of protein expression during therapy. D, Representative immunocytochemical analysis of PKCalpha protein expression (green signal) in responder and non-responder MDS patients during DFX therapy. Only non-responders show an increase of protein expression during therapy. Original magnification ×600. Nuclei are visualized by DAPI staining (blue signal). At least 10 different fields were observed

H_2-DCFDA, which accumulates within the cell and becomes fluorescent upon oxidation, there was an increase of 15% in ROS production, as compared with untreated cells. In contrast, DFX was able to completely reset the ROS production, counteracting the $FeCl_3$ effect. Of note, the Delta between fluorescence intensity decrease observed in $FeCl_3$-pretreated cells after DFX exposition (53.02% − 0.58% = 52.44%) was higher than the one observed in the untreated samples (38.82% − 0.05% = 38.77%), so that DFX-induced reduction of ROS was more marked in $FeCl_3$-pretreated cells. This effect was cell line-dependent, as THP-1 cells were not affected. That is why we did not test any inositide signaling or gene/protein expression changes with DFX in THP-1 cells, and all subsequent analyses were carried out only on K562 cells. Moreover, the DFX effect on the decrease of ROS was not due to a quenching phenomenon, as shown by both ROS analysis and CD71 expression during administration of different concentrations of H_2O_2 and $FeCl_3$, but could probably be linked to a direct effect of DFX on ROS production, whose functional role is still controversial,[56] as well as to a direct and non-specific DFX-induced change in the cell oxidative status, as reported in neutrophils.[57] As for inositide analyses, PI-PLCbeta1/Cyclin D3/PKCalpha signaling was increased only in $FeCl_3$-treated cells, while it was reduced after exposition to DFX alone and the combination treatment.

PI-PLCbeta1/Cyclin D3/PKCalpha signaling is interconnected with the Akt pathway, that in turn has been associated with ROS and cytokine secretion to regulate inflammation and oxidative stress in leukemia.[58] That is why we also analyzed autonomous changes in 12 cytokines commonly secreted by K562 and hematopoietic stem cells, to see whether the ROS production induced by $FeCl_3$ and DFX (that have a clear effect on K562 erythroleukemia cells) could also be able to change cytokine secretion in the same cells, possibly affecting specific inositide targets. In fact, IL-1A can interact with mTOR or activate PKCalpha to regulate ROS production,[59-61] while IL-2 increases the ROS production and is implicated in inositide signaling via Akt/mTOR pathway.[62-64] Our cytokine and protein analysis on K562 cells showed that the secretion of IL-1A and IL-2, as well as the level of Akt/mTOR activation, could be related to a specific response to $FeCl_3$ and DFX, thus confirming the involvement of inositide pathways in cytokine signaling and DFX response. In fact, although the reduction of IL-1A and IL-2 induced by the combination of DFX and $FeCl_3$ was not statistically significant, the cytokine changes can have an important downstream biological effect on inositide signaling, as shown by the reduction of Akt and mTOR phosphorylation.

Interestingly, the treatment of our K562 cells with $FeCl_3$ alone could imitate the condition of MDS non-responder patients, where an accumulation of iron is present. Conversely, K562 cells treated with $FeCl_3$ and DFX could mimic the responder MDS cases, that are subjected and positively respond to both iron accumulation and DFX therapy. Stemming from these premises, we further examined PI-PLCbeta1/Cyclin D3/PKCalpha signaling in a small series of MDS patients who received ICT with DFX. In our case series, a subgroup of subjects showed a favorable hematologic response and, consequently, underwent the discontinuation of transfusions and a significant reduction of serum ferritin. In contrast, the remaining patients did not show any hematologic response and continued to show transfusion-dependence, leading to high levels of serum ferritin, likely stimulating iron-induced oxidative stress. Our small group of patients was balanced, with 50% of responder and 50% of non-responder patients respectively and, although it does not reflect the percentage of responder patients in the real world setting, it was useful for our study to preliminarly perform ex vivo studies on DFX effect in a balanced population. Also a mutational analysis on our MDS patients at baseline was performed. Our next generation sequencing analysis, although obtained from a very small number of cases, could not yet predict any effect of ICT from baseline mutations, but was in accordance with a recent study showing that the number of mutations at baseline, and not the specific type of gene mutation, correlated with response and was lower in DFX responders compared to resistant patients.[49] Moreover, the same study reported that a low number of somatic mutations in bone marrow progenitors could contribute also to the positive

effects of ICT regarding the overall haematopoietic function in MDS, confirming the positive prognostic effect of a lower mutation burden in baseline MDS.[49]

As for inositides, our findings show that responder MDS patients display baseline higher levels of PI-PLCbeta1/Cyclin D3/PKCalpha mRNAs, as compared with both non-responder patients and a pool of healthy subjects. This data, even if it has to be confirmed on a larger series of patients, might be used to identify a subgroup of patients who are more likely to show a favorable hematological response to ICT. Moreover, after ICT, inositide signaling was clearly increased only in non-responder patients, who exhibited higher gene and protein expression of PI-PLCbeta1, as well as of its downstream targets Cyclin D3 and PKCalpha, all associated with cell cycle regulation and oxidative stress. In contrast, in responder subjects, the gene and protein expression of inositide signaling molecules remained almost constant after ICT, as compared with baseline. Therefore, both the presence of a peculiar molecular gene expression profile at baseline and of different patterns of molecular response of inositides to DFX hints at a role for PI-PLCbeta1 and PI-PLCbeta1-dependent signaling as molecular targets in iron-induced oxidative stress. Although apparently the gene expression changes in MDS responder patients appear to be opposite to the changes identified in K562 cells, the trend of K562 cells and patients' samples are comparable. In fact, the data reported for both K562 cells and patients' samples come from a relative quantitation analysis, in which untreated cells and healthy subjects are used as a reference. Therefore, if we compare the amount of mRNA within patients' samples during therapy, and we compare it with K562 cells' behavior during treatment, we would see that responder patients during DFX therapy show a reduction of gene expression (therapy vs baseline), and the same happens in K562 cells treated with $FeCl_3$ + DFX (as compared with CTRL). In contrast, non-responder patients during therapy show an increase of gene expression (therapy vs baseline), and the same happens in K562 cells treated only with $FeCl_3$ (as compared with CTRL).

Interestingly, although tested on a very small number of cells and samples, there was an apparent difference in PI-PLCbeta1/Cyclin D3/PKCalpha localization between baseline and therapy, that was also partially confirmed by our analyses on K562 cell line. The apparent nuclear localization of inositides during treatment could hint at a specific involvement of this signaling pathway during oxidative stress, that could be linked to a specific regulation of hematopoietic differentiation and needs to be further investigated, first in a larger number of patients' cells, then in other in vitro experimental models.

We are indeed aware that in this study we analyzed a very small number of MDS patients, and larger studies are warranted to confirm these preliminary data. Nevertheless, our results show for the first time that the expression of PI-PLCbeta1, Cyclin D3 and PKCalpha is directly associated with iron-induced oxidative stress and ROS production in both MDS and hematopoietic cells. As PI-PLCbeta1 is upstream Cyclin D3 and PKCalpha, it could become an important novel target for the development of specific innovative personalized therapies based on the reduction of oxidative stress and ROS production. Moreover, PI-PLCbeta1 quantitation could lead to a better comprehension of the mechanisms underlying the MDS pathogenesis and become a novel molecular marker in ICT, possibly allowing the early identification of patients likely to be refractory to DFX therapy.

ACKNOWLEDGMENTS

This work was supported by grants from the Italian Ministry of Education, University and Research–Research Projects of National Interest and Intesa San Paolo Foundation. AP and JB are supported by Blood Cancer UK (grant 13042).

CONFLICT OF INTEREST

The authors declare no competing financial interests.

AUTHOR CONTRIBUTIONS

A. Cappellini, S. Mongiorgi, C. Finelli, L. Cocco, M.Y. Follo: Designed research; A. Cappellini, S. Mongiorgi, A. Fazio, M.V. Marvi, M.Y. Follo: Performed research; C. Finelli, S. Ratti, A.M. Billi, P.-G. Suh, J.A. McCubrey, L. Manzoli: Contributed new reagents or analytic tools; C. Finelli, A. Curti, V. Salvestrini, A. Pellagatti, J. Boultwood: Provided and analyzed clinical samples; A. Cappellini, S. Mongiorgi, C. Finelli, A. Fazio, L. Cocco, M.Y. Follo: Analyzed data; A. Cappellini, S. Mongiorgi, C. Finelli, L. Cocco, M.Y. Follo: Wrote the paper; All authors revised the paper critically and approved the final version.

REFERENCES

1. Manzoli L, Billi AM, Gilmour RS, et al. Phosphoinositide signaling in nuclei of Friend cells: tiazofurin down-regulates phospholipase C beta 1. *Cancer Res*. 1995;55:2978-2980.
2. Ratti S, Ramazzotti G, Faenza I, et al. Nuclear inositide signaling and cell cycle. *Adv Biol Regul*. 2018;67:1-6.
3. Faenza I, Bavelloni A, Fiume R, et al. Up-regulation of nuclear PLCbeta1 in myogenic differentiation. *J Cell Physiol*. 2003;195:446-452.
4. Faenza I, Billi AM, Follo MY, et al. Nuclear phospholipase C signaling through type 1 IGF receptor and its involvement in cell growth and differentiation. *Anticancer Res*. 2005;25:2039-2041.
5. Follo MY, Mongiorgi S, Finelli C, et al. Nuclear inositide signaling in myelodysplastic syndromes. *J Cell Biochem*. 2010;109:1065-1071.
6. Ramazzotti G, Faenza I, Fiume R, et al. The physiology and pathology of inositide signaling in the nucleus. *J Cell Physiol*. 2011;226:14-20.
7. Poli A, Fiume R, Baldanzi G, et al. Nuclear localization of diacylglycerol kinase alpha in K562 cells is involved in cell cycle progression. *J Cell Physiol*. 2017;232:2550-2557.

8. Poli A, Mongiorgi S, Cocco L, Follo MY. Protein kinase C involvement in cell cycle modulation. *Biochem Soc Trans*. 2014;42:1471-1476.
9. Ratti S, Mongiorgi S, Ramazzotti G, et al. Nuclear inositide signaling via phospholipase C. *J Cell Biochem*. 2017;118:1969-1978.
10. Ratti S, Follo MY, Ramazzotti G, et al. Nuclear phospholipase C isoenzyme imbalance leads to pathologies in brain, hematologic, neuromuscular, and fertility disorders. *J Lipid Res*. 2019;60:312-317.
11. Lo Vasco VR, Calabrese G, Manzoli L, et al. Inositide-specific phospholipase c beta1 gene deletion in the progression of myelodysplastic syndrome to acute myeloid leukemia. *Leukemia*. 2004;18:1122-1126.
12. Ratti S, Mongiorgi S, Rusciano I, Manzoli L, Follo MY. Glycogen Synthase Kinase-3 and phospholipase C-beta signalling: roles and possible interactions in myelodysplastic syndromes and acute myeloid leukemia. *Biochim Biophys Acta Mol Cell Res*. 2020;1867:118649.
13. Xian J, Owusu Obeng E, Ratti S, et al. Nuclear inositides and inositide-dependent signaling pathways in myelodysplastic syndromes. *Cells*. 2020;9:697.
14. Follo MY, Russo D, Finelli C, et al. Epigenetic regulation of nuclear PI-PLCbeta1 signaling pathway in low-risk MDS patients during azacitidine treatment. *Leukemia*. 2012;26:943-950.
15. Follo MY, Mongiorgi S, Clissa C, et al. Activation of nuclear inositide signalling pathways during erythropoietin therapy in low-risk MDS patients. *Leukemia*. 2012;26:2474-2482.
16. Follo MY, Finelli C, Mongiorgi S, et al. Synergistic induction of PI-PLCbeta1 signaling by azacitidine and valproic acid in high-risk myelodysplastic syndromes. *Leukemia*. 2011;25:271-280.
17. Poli A, Ratti S, Finelli C, et al. Nuclear translocation of PKC-alpha is associated with cell cycle arrest and erythroid differentiation in myelodysplastic syndromes (MDSs). *FASEB J*. 2018;32:681-692.
18. Forciniti S, Greco L, Grizzi F, Malesci A, Laghi L. Iron metabolism in cancer progression. *Int J Mol Sci*. 2020;21:2257.
19. Guida M, Maraldi T, Beretti F, Follo MY, Manzoli L, De Pol A. Nuclear Nox4-derived reactive oxygen species in myelodysplastic syndromes. *Biomed Res Int*. 2014;2014:456937.
20. Keune WJ, Jones DR, Divecha N. PtdIns5P and Pin1 in oxidative stress signaling. *Adv Biol Regul*. 2013;53:179-189.
21. Poli A, Zaurito AE, Abdul-Hamid S, Fiume R, Faenza I, Divecha N. Phosphatidylinositol 5 Phosphate (PI5P): from behind the scenes to the front (nuclear) stage. *Int J Mol Sci*. 2019;20:2080.
22. Suire S, Baltanas FC, Segonds-Pichon A, et al. Frontline science: TNF-alpha and GM-CSF1 priming augments the role of SOS1/2 in driving activation of Ras, PI3K-gamma, and neutrophil proinflammatory responses. *J Leukoc Biol*. 2019;106:815-822.
23. Leslie NR, Bennett D, Lindsay YE, Stewart H, Gray A, Downes CP. Redox regulation of PI 3-kinase signalling via inactivation of PTEN. *EMBO J*. 2003;22:5501-5510.
24. Casciaro F, Beretti F, Zavatti M, et al. Nuclear Nox4 interaction with prelamin A is associated with nuclear redox control of stem cell aging. *Aging (Albany NY)*. 2018;10:2911-2934.
25. Zeitz MJ, Malyavantham KS, Seifert B, Berezney R. Matrin 3: chromosomal distribution and protein interactions. *J Cell Biochem*. 2009;108:125-133.
26. Jayavelu AK, Moloney JN, Böhmer FD, Cotter TG. NOX-driven ROS formation in cell transformation of FLT3-ITD-positive AML. *Exp Hematol*. 2016;44:1113-1122.
27. Song MG, Ryoo IG, Choi HY, et al. NRF2 signaling negatively regulates phorbol-12-myristate-13-acetate (PMA)-induced differentiation of human monocytic U937 cells into pro-inflammatory macrophages. *PLoS One*. 2015;10:e0134235.
28. Leitch HA, Gattermann N. Hematologic improvement with iron chelation therapy in myelodysplastic syndromes: Clinical data, potential mechanisms, and outstanding questions. *Crit Rev Oncol Hematol*. 2019;141:54-72.
29. Zuo Y, Xiang B, Yang J, et al. Oxidative modification of caspase-9 facilitates its activation via disulfide-mediated interaction with Apaf-1. *Cell Res*. 2009;19:449-457.
30. Hartmann J, Braulke F, Sinzig U, et al. Iron overload impairs proliferation of erythroid progenitors cells (BFU-E) from patients with myelodysplastic syndromes. *Leuk Res*. 2013;37:327-332.
31. Bowen D, Wang L, Frew M, Kerr R, Groves M. Antioxidant enzyme expression in myelodysplastic and acute myeloid leukemia bone marrow: further evidence of a pathogenetic role for oxidative stress? *Haematologica*. 2003;88:1070-1072.
32. Novotna B, Bagryantseva Y, Siskova M, Neuwirtova R. Oxidative DNA damage in bone marrow cells of patients with low-risk myelodysplastic syndrome. *Leuk Res*. 2009;33:340-343.
33. Ghoti H, Fibach E, Merkel D, Perez-Avraham G, Grisariu S, Rachmilewitz EA. Changes in parameters of oxidative stress and free iron biomarkers during treatment with deferasirox in iron-overloaded patients with myelodysplastic syndromes. *Haematologica*. 2010;95:1433-1434.
34. Angelucci E, Santini V, Di Tucci AA, et al. Deferasirox for transfusion-dependent patients with myelodysplastic syndromes: safety, efficacy, and beyond (GIMEMA MDS0306 Trial). *Eur J Haematol*. 2014;92:527-536.
35. Nolte F, Hochsmann B, Giagounidis A, et al. Results from a 1-year, open-label, single arm, multi-center trial evaluating the efficacy and safety of oral Deferasirox in patients diagnosed with low and int-1 risk myelodysplastic syndrome (MDS) and transfusion-dependent iron overload. *Ann Hematol*. 2013;92:191-198.
36. Gattermann N, Finelli C, Della Porta M, et al. Hematologic responses to deferasirox therapy in transfusion-dependent patients with myelodysplastic syndromes. *Haematologica*. 2012;97:1364-1371.
37. Messa E, Carturan S, Maffe C, et al. Deferasirox is a powerful NF-kappaB inhibitor in myelodysplastic cells and in leukemia cell lines acting independently from cell iron deprivation by chelation and reactive oxygen species scavenging. *Haematologica*. 2010;95:1308-1316.
38. Manzoli L, Mongiorgi S, Clissa C, et al. Strategic role of nuclear inositide signalling in myelodysplastic syndromes therapy. *Mini Rev Med Chem*. 2014;14:873-883.
39. Cermak J, Jonasova A, Vondrakova J, Cervinek L, Belohlavkova P, Neuwirtova R. A comparative study of deferasirox and deferiprone in the treatment of iron overload in patients with myelodysplastic syndromes. *Leuk Res*. 2013;37:1612-1615.
40. Harmening D, Baldwin AJ, Sohmer PR. *Modern Blood Banking & Transfusion Practices*. Philadelphia, PA: F.A. Davis; 1983.
41. Cappellini MD. Exjade(R) (deferasirox, ICL670) in the treatment of chronic iron overload associated with blood transfusion. *Ther Clin Risk Manag*. 2007;3:291-299.
42. Vardiman JW, Thiele J, Arber DA, et al. The 2008 revision of the World Health Organization (WHO) classification of myeloid neoplasms and acute leukemia: rationale and important changes. *Blood*. 2009;114:937-951.

43. Greenberg P, Cox C, LeBeau MM, et al. International scoring system for evaluating prognosis in myelodysplastic syndromes. *Blood*. 1997;89:2079-2088.
44. Cheson BD, Greenberg PL, Bennett JM, et al. Clinical application and proposal for modification of the International Working Group (IWG) response criteria in myelodysplasia. *Blood*. 2006;108:419-425.
45. Pellagatti A, Roy S, Di Genua C, et al. Targeted resequencing analysis of 31 genes commonly mutated in myeloid disorders in serial samples from myelodysplastic syndrome patients showing disease progression. *Leukemia*. 2016;30:247-250.
46. Follo MY, Pellagatti A, Armstrong RN, et al. Response of high-risk MDS to azacitidine and lenalidomide is impacted by baseline and acquired mutations in a cluster of three inositide-specific genes. *Leukemia*. 2019;33:2276-2290.
47. Cocco L, Finelli C, Mongiorgi S, et al. An increased expression of PI-PLCbeta1 is associated with myeloid differentiation and a longer response to azacitidine in myelodysplastic syndromes. *J Leukoc Biol*. 2015;98:769-780.
48. Chan S, Chan GC, Ye J, Lian Q, Chen J, Yang M. Thrombopoietin protects cardiomyocytes from iron-overload induced oxidative stress and mitochondrial injury. *Cell Physiol Biochem*. 2015;36:2063-2071.
49. Fabiani E, Calabrese C, Niscola P, et al. Mutational profile and haematological response to iron chelation in myelodysplastic syndromes (MDS). *Br J Haematol*. 2019;185:954-957.
50. Mongiorgi S, Finelli C, Yang YR, et al. Inositide-dependent signaling pathways as new therapeutic targets in myelodysplastic syndromes. *Expert Opin Ther Targets*. 2016;20:677-687.
51. Mongiorgi S, Follo MY, Yang YR, et al. Selective activation of nuclear PI-PLCbeta1 during normal and therapy-related differentiation. *Curr Pharm Des*. 2016;22:2345-2348.
52. Follo MY, Marmiroli S, Faenza I, et al. Nuclear phospholipase C beta1 signaling, epigenetics and treatments in MDS. *Adv Biol Regul*. 2013;53:2-7.
53. Tataranni T, Mazzoccoli C, Agriesti F, et al. Deferasirox drives ROS-mediated differentiation and induces interferon-stimulated gene expression in human healthy haematopoietic stem/progenitor cells and in leukemia cells. *Stem Cell Res Ther*. 2019;10:171.
54. Chen YL, Kan WM. Down-regulation of superoxide dismutase 1 by PMA is involved in cell fate determination and mediated via protein kinase D2 in myeloid leukemia cells. *Biochim Biophys Acta*. 2015;1853:2662-2675.
55. Nocka KH, Pelus LM. Cell cycle specific effects of deferoxamine on human and murine hematopoietic progenitor cells. *Cancer Res*. 1988;48:3571-3575.
56. Jiménez-Solas T, López-Cadenas F, Aires-Mejía I, et al. Deferasirox reduces oxidative DNA damage in bone marrow cells from myelodysplastic patients and improves their differentiation capacity. *Br J Haematol*. 2019;187:93-104.
57. Saigo K, Kono M, Takagi Y, et al. Deferasirox reduces oxidative stress in patients with transfusion dependency. *J Clin Med Res*. 2013;5:57-60.
58. Silva A, Gírio A, Cebola I, Santos CI, Antunes F, Barata JT. Intracellular reactive oxygen species are essential for PI3K/Akt/mTOR-dependent IL-7-mediated viability of T-cell acute lymphoblastic leukemia cells. *Leukemia*. 2011;25:960-967.
59. Garlanda C, Mantovani A. Ligands and receptors of the interleukin-1 family in immunity and disease. *Front Immunol*. 2013;4:396.
60. Gozali MV, Yi F, Zhang JA, et al. Photodynamic therapy inhibit fibroblast growth factor-10 induced keratinocyte differentiation and proliferation through ROS in fibroblast growth factor receptor-2b pathway. *Sci Rep*. 2016;6:27402.
61. Zhu G, Liu X, Fang Y, et al. Increased mTOR cancels out the effect of reduced Xbp-1 on antibody secretion in IL-1α-deficient B cells. *Cell Immunol*. 2018;328:9-17.
62. Kelly E, Won A, Refaeli Y, Van Parijs L. IL-2 and related cytokines can promote T cell survival by activating AKT. *J Immunol*. 2002;168:597-603.
63. Bae J, Park D, Lee YS, Jeoung D. Interleukin-2 promotes angiogenesis by activation of Akt and increase of ROS. *J Microbiol Biotechnol*. 2008;18:377-382.
64. Zhang J, Wang X, Vikash V, et al. ROS and ROS-mediated cellular signaling. *Oxid Med Cell Longev*. 2016;2016:4350965.

SUPPORTING INFORMATION

Additional supporting information may be found online in the Supporting Information section.

How to cite this article: Cappellini A, Mongiorgi S, Finelli C, et al. Phospholipase C beta1 (PI-PLCbeta1)/Cyclin D3/protein kinase C (PKC) alpha signaling modulation during iron-induced oxidative stress in myelodysplastic syndromes (MDS). *The FASEB Journal*. 2020;34:15400–15416. https://doi.org/10.1096/fj.202000933RR